Sensors and Materials, Vol. 37, No. 4 (2025) 1753–1764
MYU Tokyo

S & M 4015

Envelope Sensor Design for Partial Discharge Signals of High-voltage Power Apparatus

Cheng-Chien Kuo,[1] Yu-Ming Liu,[1] Hung-Cheng Chen,[2*] and Ting-Jui Yang[2]

[1]Department of Electrical Engineering, National Taiwan University of Science and Technology, No. 43, Sec. 4, Keelung Rd., Da'an Dist., Taipei City 106335, Taiwan (R.O.C.)
[2]Department of Electrical Engineering, National Chin-Yi University of Technology, No.57, Sec. 2, Zhongshan Rd., Taiping Dist., Taichung 411030, Taiwan (R.O.C.)

(Received November 11, 2024; accepted April 14, 2025)

Keywords: partial discharge, envelope sensor, high-pass filter circuit, signal amplifier circuit, envelope detection circuit

The detection of partial discharge (PD) is an effective way to evaluate the insulation of a power system for the early discovery of failures. It ensures the safety, reliability, and economic operation of equipment. In this study, an envelope sensor was designed for PD signals. It consisted of a high-pass filter circuit, a signal amplifier circuit, and an envelope detection circuit. PD oscillatory signals were converted into low-frequency impulse envelope signals to effectively identify the peak voltage and the phase of occurrence as important data for the PD diagnosis and identification of failure patterns. To test the validity of the envelope sensor, corona discharge and surface discharge signals were generated using various PD experimental models. The coupling of a high-frequency current transformer was introduced to acquire PD signals. Data acquisition and signal analysis were performed using an oscilloscope after the signals were processed by the detection system. The experiment conducted revealed that the proposed envelope sensor was effective for measuring the impulse envelope of PD oscillations. The peak voltage and the phase of occurrence were identified, and the output impulse envelope signals were of low frequency, which contributed to the subsequent signal acquisition and analysis.

1. Introduction

The demand for electric power increases with the advance of technology. The state and quality of power equipment are a crucial link to keeping the power system up and running. Recent statistics have shown that a large portion of high-voltage equipment damage was a result of insulation faults, which can originate from human or natural factors.[1–3] One human factor is the inappropriate operation of machines, which may cause insignificant defects during the production process, whereas humidity, temperature, and heat are examples of natural factors. At present, the most effective way to detect insulation faults is the measurement of partial discharge (PD). This approach provides important indicators for the insulation inside high-voltage equipment.

*Corresponding author: e-mail: hcchen@ncut.edu.tw
https://doi.org/10.18494/SAM5468

ISSN 0914-4935
https://myukk.org/

It allows not only for obtaining important information about the internal insulation of equipment but also for the early prevention of equipment damage and the extension of service life. PD detection has a wide range of applications. PD can exist in, for example, gas insulation switchgears, transformers, and high-voltage motors.[4,5] PD detection equipment is expensive on the order of hundreds of thousands to millions of NT dollars. It is not an affordable solution for small businesses. On the other hand, if a self-developed detection instrument can measure PD signals with acceptable accuracy, this can be a favorable solution in terms of budget and fault identification.

An envelope sensor was designed in this study for PD signals. The detection started by screening out low-frequency noises with a high-pass filter. High-frequency signals were amplified by a high-bandwidth current feedback amplifier circuit. An envelope detection circuit converted PD oscillatory signals into low-frequency impulse envelope signals for subsequent signal acquisition and analysis.[6,7] The novelty of this study is to convert a high-frequency PD signal into a low-frequency envelope signal, which can significantly reduce the cost of signal acquisition equipment.

2. Envelope Sensor Design

The envelope sensor for PD signals consists of a high-pass filter circuit, a signal amplifier circuit, and an envelope detection circuit, each of which is described as follows:

2.1 High-pass filter circuit

It is common to encounter a considerable amount of noise during field testing. Therefore, a high-pass filter is added to screen out low-frequency noises for higher accuracy in measurement results. To make the acquired PD signals with longer oscillations for the ease of identifying PD signals and considering the circuit costs and service life, a passive filter was used as the high-pass filter. The circuit diagram is shown in Fig. 1(a). Figure 1(b) provides the frequency response with the cut-off frequency f_c = 6 MHz. Table 1 shows the simulation results vs actual measurements of the circuit.

It is clear in the frequency response diagram in Fig. 1(b) that the output signals were 0 for 3–4 MHz in the simulation results, and that all signals pass at 6 MHz. As shown by the actual measurements of the filter, all signals failed to pass at around 3–5 MHz, a few of the signals passed at 6 MHz, and all of them passed at 3–4 MHz. This is probably because of the minor impedance existing in the cables and wiring of the actual circuit. At low frequencies, ωL was very small and therefore produced a minimal effect. On the other hand, at high frequencies, ωL was large,[8] resulting in circuit decay by −3 dB. As shown in the actual measurements, the effects of the filter circuit met the requirements of the study.

2.2 Signal amplifier circuit

The period of PD signals usually falls between 60 ns and 30 μs. For this study, the current feedback amplifier AD8012 was chosen as the amplification circuit of the system to be able to

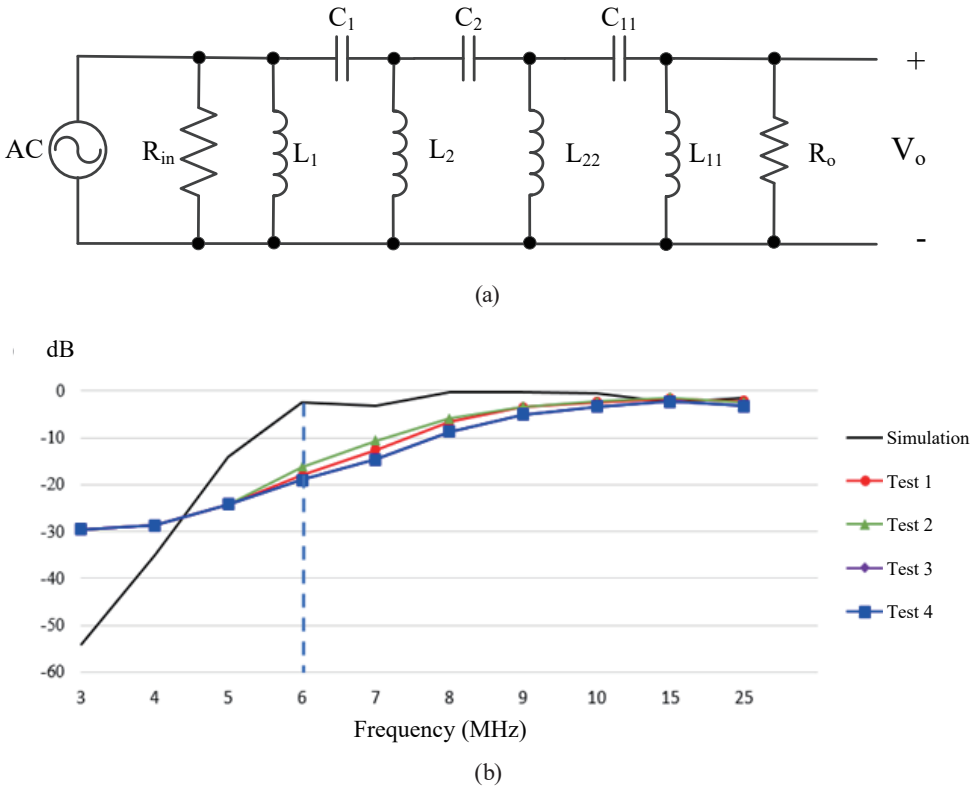

Fig. 1. (Color online) High-pass filter: (a) circuit diagram and (b) frequency response.

Table 1
Comparison of simulation and actual measurement results.

Input frequency (Hz)	Simulation result (dB)	Test1	Test2	Test3	Test4
3 M	−54.1	−29.54	−29.54	−29.54	−29.54
4 M	−35.3	−28.62	−28.62	−28.62	−28.62
5 M	−17.7	−24.17	−24.17	−24.17	−24.17
6 M	−1.69	−17.97	−16.17	−16.17	−19
7 M	−1.15	−12.56	−12.21	−10.62	−14.6
8 M	−0.28	−6.57	−6.57	−5.91	−8.74
9 M	−0.35	−3.52	−3.72	−3.32	−5.03
10 M	−0.56	−2.4	−2.78	−2.22	−3.3
15 M	−1.41	−1.61	−1.43	−1.43	−2.31
25 M	−1.45	−2.16	−2.35	−2.35	−3.24

use fast signals for the complete amplification of characteristics. This amplifier was chosen for its low distortion and extensive bandwidth. The bandwidth can reach up to 350 MHz at 100% gain. Figure 2(a) shows the wiring diagram with a gain factor of 10. The results of actual measurements of the frequency response are given in Fig. 2(b), as the bandwidth can be as large as 40 MHz. It is observed from the frequency response in Fig. 2(b) that the amplification gain factor remained at 10 times when the frequency was kept below 2 MHz. However, the gain factor started to decrease after 2.2 MHz. The gain factor of the current feedback amplifier decreases with increasing frequency in the relation expressed as

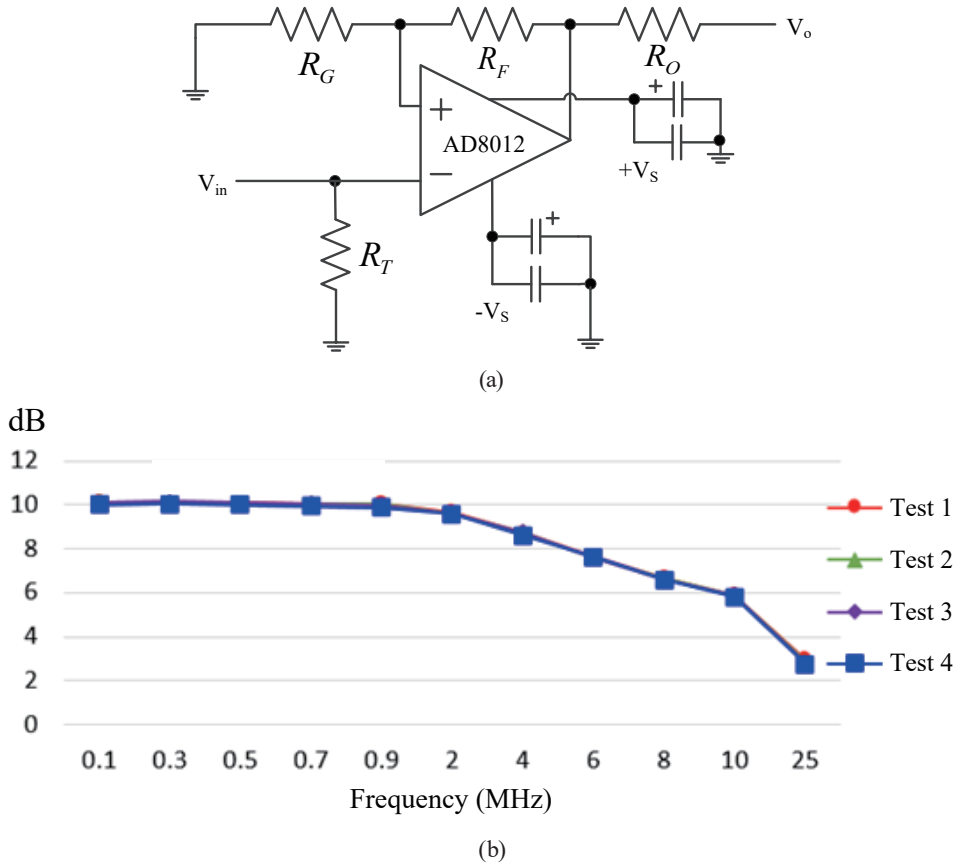

Fig. 2. (Color online) Signal amplifier circuit: (a) circuit diagram and (b) results of actual measurements of frequency response.

$$A(jf) = \frac{1 + \frac{R_G}{R_F}}{1 + j(f / f_A)}, \tag{1}$$

where $A(jf)$ is the closed loop gain factor of the amplifier, $1 + R_G/R_F$ is the transresistance gain, and f_A is the closed loop bandwidth. With increasing frequency, the magnification of the amplifier decreased.

2.3 Envelope detection circuit

High-frequency signals were the input of the envelope detection circuit. The output waveform was the envelope of raw signals. Figure 3 shows the envelope detection circuit designed for this study. The diode in the circuit rectifies the PD signal, and the resistor–capacitor (RC) circuit allows the output waveform to follow the envelope of the sinusoid. In the envelope detection circuit, C_e is 470 pF and R_e is 50 kΩ. The bandwidth of the detected modulation waveform is

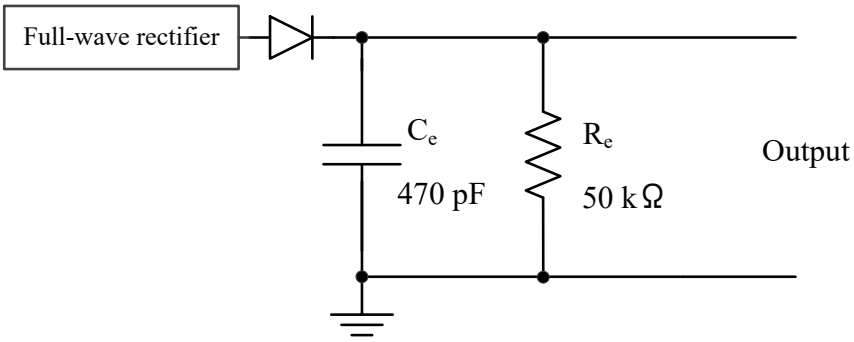

Fig. 3. Envelope detection circuit.

much less than f_c (carrier frequency), as determined using Eq. (2). A full-wave rectifier at the front end of the circuit converted the signals into DC oscillatory signals. At the rear end, a 10-kHz low-pass filter smoothed out the final output results.[9,10] The low-pass filter generated ripples and kept the following envelope output. The frequencies of the final output results were maintained below 10 kHz. The typical waveforms measured by the envelope detection circuit are provided in Fig. 4(a), where the yellow channel indicates the raw PD signals of input at approximately 14.4 MHz, the red channel the full-wave rectified output at 30.94 MHz, the blue channel the output of the envelope detection circuit at 4.88 kHz, and the green channel the benchmark signal of utility power. Figure 4(b) shows the enlarged waveforms. It is proven that the envelope sensor designed for this study can accurately convert raw PD oscillatory waves into impulse envelope signals, achieving the design goal of the study.

$$f_c = \frac{1}{2\pi RC} = \frac{1}{2\pi * 50\,\mathrm{k\Omega} * 470\,\mathrm{pF}} = 6.7\ \mathrm{kHz} \tag{2}$$

Figure 5 shows one PD pulse signal process result obtained using our self-developed detection system. The yellow line is the original oscillating signal measured by a high-frequency current transformer (HFCT). The red line represents the signal processed after the high-pass filter and amplifier. The blue line is the signal after the rectification process. The green line indicates the result of envelope detection.

3. PD Test Platform

Custom-made PD defect samples were used for the measurement and testing of PD signals. PD signals are oscillatory current signals with high frequencies. The acquired raw signals have high frequencies. Therefore, the detection equipment should be able to detect such signals at high frequencies, resulting in its high cost. The envelope sensor proposed in this study converted high-frequency oscillatory signals into low-frequency impulse signals for subsequent signal acquisition and analysis at a rather affordable cost.

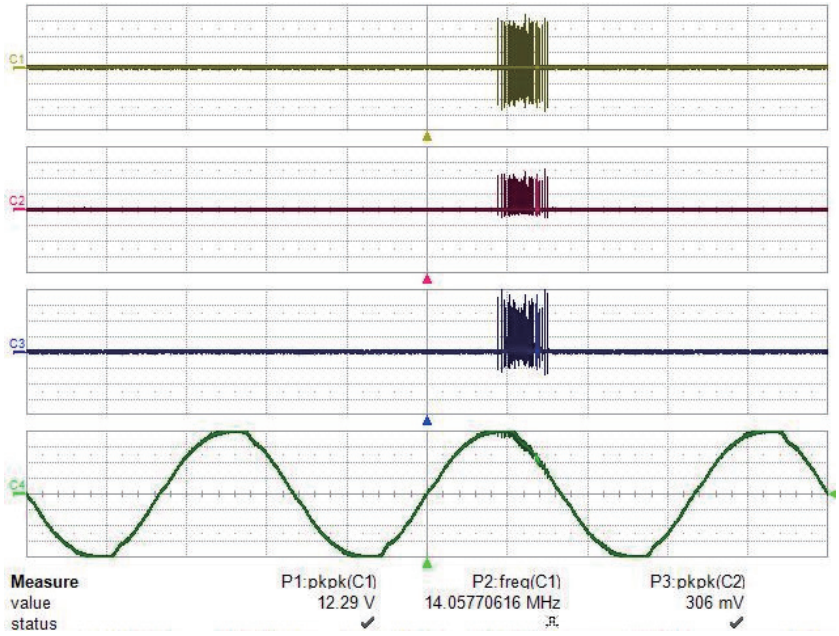

(a)

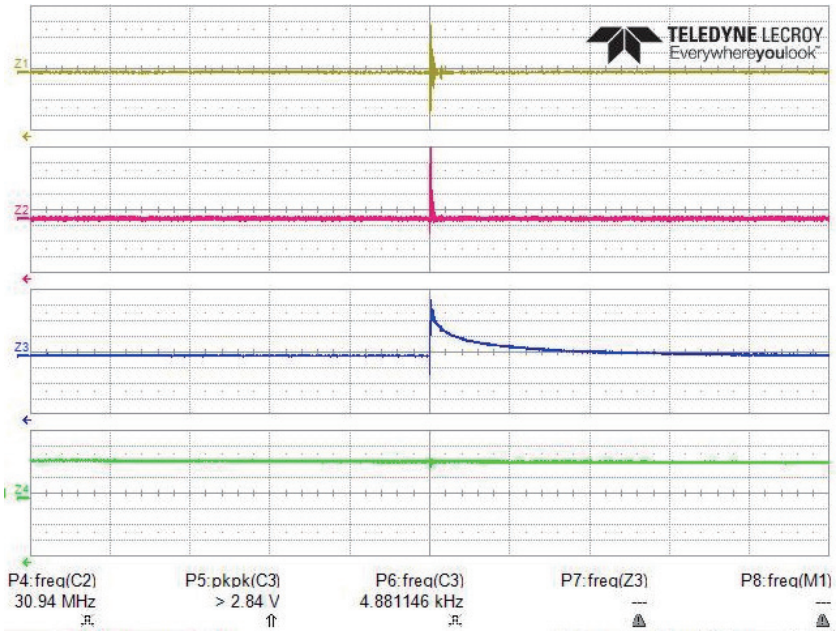

(b)

Fig. 4. (Color online) Typical waveforms measured by envelope detection circuit. (a) Envelope output by every discharge and (b) enlarged waveform of one of the envelopes.

3.1 Actual samples of defect model

There are two types of discharge commonly seen in high-voltage equipment according to a literature review, namely, corona discharge and surface discharge. For these types, four

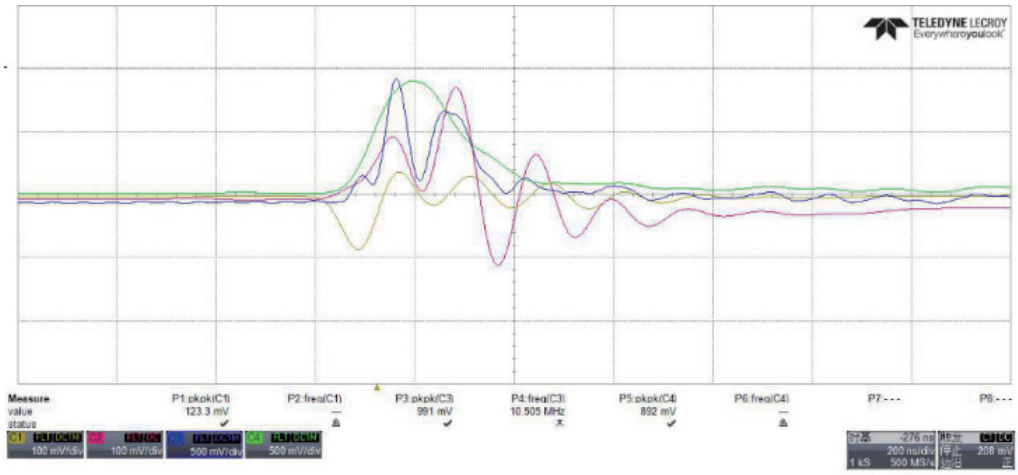

Fig. 5. (Color online) Processing results of PD pulse signal using the self-developed detection system.

discharge defect models were constructed. The PD experiment model is shown in Fig. 6, the test platform in Fig. 6(a), and the discharge defect samples in Fig. 6(b).[11–15] The specifications of the four discharge defect samples are shown below.

(1) Needle-to-plane model. A 4-mm-diameter copper stick is lathed at one end to a 0.5-mm-diameter cone needle, which is 6 cm away from the plane.
(2) Needle-to-plane model. A 4-mm-diameter copper stick is lathed at one end to a 1-mm-diameter cone needle, which is 6 cm away from the plane.
(3) Needle-to-plane model. A 4-mm-diameter copper stick is lathed at one end to a 2-mm-diameter cone needle, which is 6 cm away from the plane.
(4) Plane-to-plane model. A 3-mm-thick epoxy layer is inserted.

3.2 Experimental process

A 0–110 V autotransformer regulated the voltage for a 110 V/24 kV high-voltage transformer, and the high voltage from the transformer was applied to the test samples. The measurement system setup is shown in Fig. 7. The voltage increase stopped when PD was observed on the test samples. The HFCT coupling was used to measure the PD signals on the test samples. The self-developed detection system consists of a high-pass filter circuit, an amplifier circuit, and an envelope detection circuit. The PD waveforms are detected using the proposed envelope sensor and transmitted to an oscilloscope for signal analysis and data storage.[16] The test process is shown in Fig. 8.

4. Measurement Results and Analysis

The defect samples were placed in the atmosphere for the discharge test. The AC voltage was increased to 200 V in steps of 10 V until discharge was observed. The PD inception voltage was approximately 8 kV with AC voltage at 60 Hz. The rise time for the discharge wave was 62 ns.

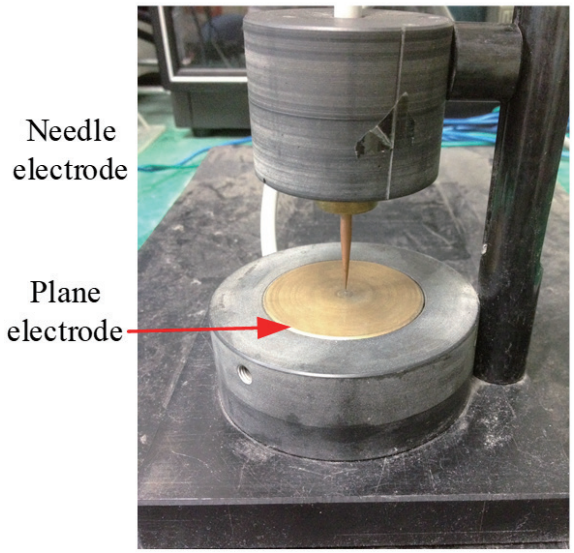

(a)

(b)

Fig. 6. (Color online) PD experimental model: (a) experimental platform and (b) experimental samples of the defect models.

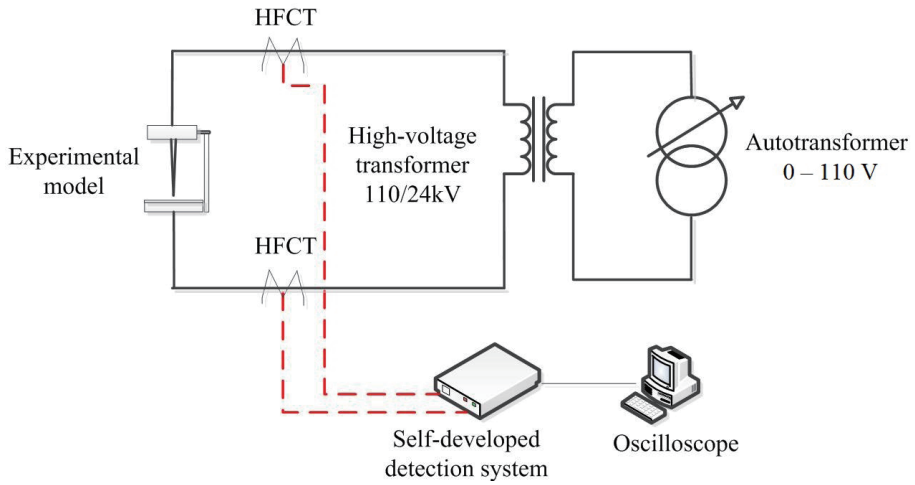

Fig. 7. (Color online) Structure of the measurement system.

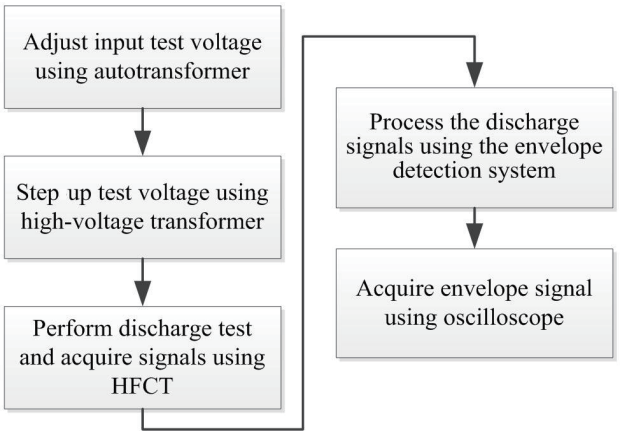

Fig. 8. (Color online) Flow chart of the experiment.

Figure 9 shows the actual waveforms measured at PD and the envelope output waveforms. On the left are the PD waveforms of the four defect samples measured by the proposed system. The yellow channel indicates the voltage signals of utility power. Three wavelengths of utility power signals were acquired as benchmarks. The blue channel indicates the impulse envelope signals acquired at the needle electrode, and the red channel indicates those acquired at the plane electrode. The signal sampling rate of the oscilloscope was 20 Msps.

A literature review suggested that the eigenvalues of the corona discharge signals were located in quadrants 1 and 3, but a few of the impulses were found in quadrants 2 and 4 occasionally. The eigenvalues of surface discharge were located in quadrants 1 and 3 as well. However, the discharge magnitudes varied and the discharge phases were dispersed. Figure 9(a) shows the corona discharge signals from a 0.5-mm-diameter copper stick to a plane electrode. It is seen on the left that there are few continuous discharges because of the small tip area, and most of the discharges are found in quadrant 3. The right panel of Fig. 9(a) shows the waveforms of quadrant 3 signals after amplification. It is clear from the figure that the peak value acquired at the needle electrode is greater than that acquired at the plane electrode. This could be due to the discharge from the needle electrode at the top to the plane electrode at the bottom. The output waves of the impulse signals are kept below 10 kHz. Figure 9(b) shows the signal diagram of the corona discharge test for the 1-mm-diameter copper stick test sample. The left panel shows that there are more discharges probably because of the larger tip area of the needle electrode, resulting in slightly dispersed discharged spots.

However, the discharges are still mostly located in quadrants 1 and 3. The right panel of Fig. 9(b) shows the waveforms of quadrant 3 signals after amplification, which are similar to those in Fig. 9(a). Figure 9(c) shows the corona discharge signals of the plane electrode test for the 2-mm-diameter copper stick. The waveforms on the left are similar to those in Fig. 9(b). The right panel of Fig. 9(c) shows the waveforms of the quadrant 3 signals after amplification. It is clear that there are more discharges from the needle electrode at the top to the plane electrode at the bottom, increasing the output envelope signal level of the needle electrode. Figure 9(d) shows the signal diagram obtained by placing a 3-mm-thick epoxy layer between two plane electrodes for

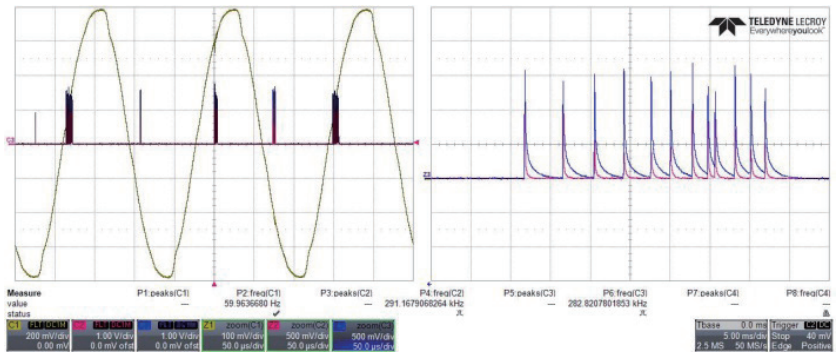

(a)

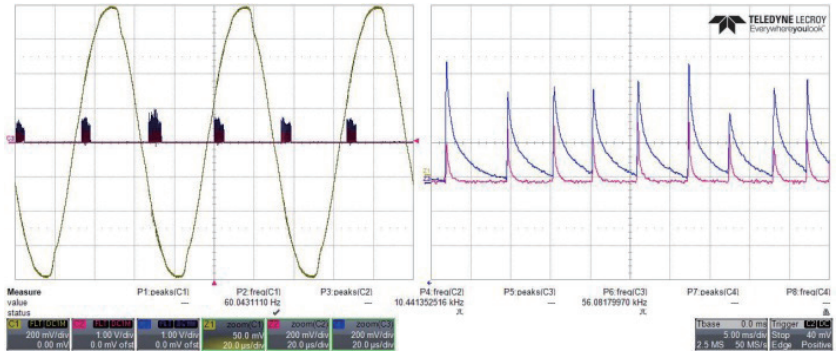

(b)

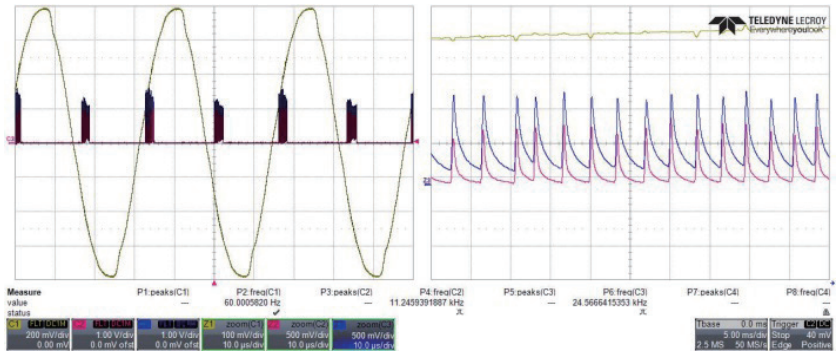

(c)

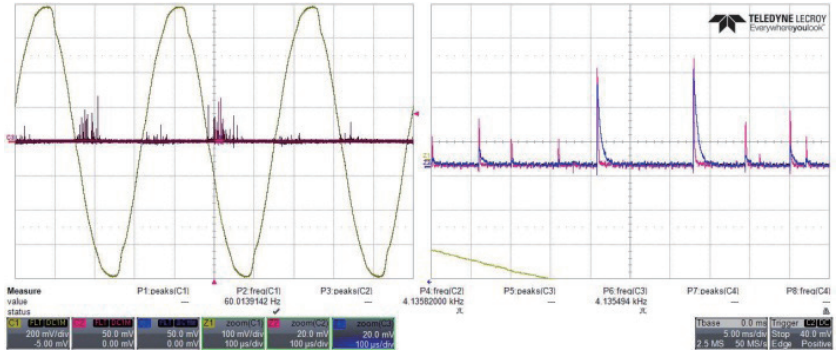

(d)

Fig. 9. (Color online) Actual PD waveforms measured and the output waveforms from the envelope sensor, (a) copper stick electrode, 0.5 mm in diameter; (b) copper stick electrode, 1 mm in diameter; (c) copper stick electrode, 2 mm in diameter; (d) epoxy layer, 3 mm in thickness placed between two plane electrodes.

the surface discharge test. It is found on the left panel that the discharge signals occur in quadrants 1 and 3, the phases of occurrence are dispersed, and discharge magnitudes vary and the magnitude in quadrant 1 is smaller than that in quadrant 3. The quadrant 3 signals are magnified on the right panel for clearer observation. It is clear that the surface discharges generate only a few large discharge envelope signals. Most of the signals are smaller, and the larger signals tend to penetrate the insulation system at any moment.

By summarizing the results above, the peak values and phases of occurrence of the raw impulse signals were found after the discharge signals were converted by the proposed envelope sensor.

5. Conclusions

An envelope sensor was developed for PD signals. The results of the experiments proved that high-frequency PD oscillatory signals were successfully converted into low-frequency impulse signals after the acquired PD signals were converted in the proposed system. The system not only identifies the PD peak voltage and phase of occurrence more effectively in the subsequent analysis but also pinpoints the type of fault in the n–q–φ diagnosis of the phase-resolved PD or the diagnosis of the three-phase amplitude relation diagram. The accuracy can be even higher once real-time monitoring is realized in the future.

PD has become the mainstream factor for detecting insulation system faults. Many detection instruments have been developed to detect the characteristics of equipment before any fault occurs, and most of these instruments are incorporated with an Internet connection capability for online monitoring. The operations of machines on site can be easily monitored and data can be collected online through the Internet. A possible topic of future studies can be the development of a remote real-time online data collection and monitoring platform based on the results of the envelope sensor proposed for receiving PD signals remotely in real time and detecting possible equipment faults as early as possible.

Acknowledgments

This research was partially supported by the National Science and Technology Council under Grant no. NSTC 113-2221-E-167-012-MY3.

References

1 H. Ma, J. C. Chan, T. K. Saha, and C. Ekanayake: IEEE Trans. Dielectr. Electr. Insul. **20** (2013) 468. https://doi.org/10.1109/TDEI.2013.6508749F
2 R. Hussein, K. B. Shaban, and A. H. El-Hag: IEEE Trans. Dielectr. Electr. Insul. **23** (2016) 1453. https://doi.org/10.1109/TDEI.2015.005532
3 J. C. Chan, H. Ma, T. K. Saha, and C. Ekanayake: IEEE Trans. Dielectr. Electr. Insul. **21** (2014) 294. https://doi.org/10.1109/TDEI.2013.003839
4 X. Bi, A. Ren, S. Li, M. Han, and Q. Li: J. Electr. Comp. Eng. **1** (2015) 294. https://doi.org/10.1155/2015/174538
5 Y. Zhang, D. Upton, A. Jaber, H. Ahmed, B. Saeed, P. Mather, P. Lazaridis, A. Mopty, C. Tachtatzis, R. Atkins, M. Judd, M. F. Q. Vieira, and I. Glover: Int. J. Distri. Sens. Net. (2015) 1. https://doi.org/10.1155/2015/438302

6 B. Sheng, C. Zhou, D. M. Hepburn, X. Dong, G. Peers, W. Zhou, and Z. Tang: IEEE Trans. Dielectr. Electr. Insul. **21** (2014) 948. https://doi.org/10.1109/TDEI.2014.6832236
7 H. C. Chen: IET Sci. Meas. Technol. **7** (2013) 77. https://doi.org/10.1049/iet-smt.2012.0078
8 R. L. Boylestad: Introductory Circuit Analysis, Global Edition (PEARSON, 2016).
9 T. Pinpart and M. Judd: IET Sci. Meas. Technol. **4** (2010) 256. https://doi.org/10.1049/iet-smt.2009.0064
10 G. Ueta, J. Wada, S. Okabe, M. Miyashita, C. Nishida, and M. Kamei: IEEE Trans. Dielectr. Electr. Insul. **19** (2012) 947. https://doi.org/10.1109/TDEI.2012.6215098
11 H. C. Chen and F. C. Gu: Expert Syst. Appl. **39** (2012) 6575. https://doi.org/10.1016/j.eswa.2011.12.044
12 F. C. Gu, H. C. Chang, and C. C. Kuo: IEEE Trans. Dielectr. Electr. Insul. **20** (2013) 1049. https://doi.org/10.1109/TDEI.2013.6571416
13 Y. Hu, F. Zhang, L. Xu, R. Tao, and Y. Wang: IET Signal Process. **10** (2016) 140. https://ieeexplore.ieee.org/document/7440944
14 C. S. Chang, J. Jin, C. Chang, T. Hoshino, M. Hanai, and N. Kobayashi: IEEE Trans. Power Delivery **20** (2005) 1363. https://doi.org/10.1109/TPWRD.2004.839187
15 M. Majidi and M. Oskuoee: Electr. Power Syst. Res. **119** (2015) 100. https://doi.org/10.1016/j.epsr.2014.09.014
16 J. Song, C. Li, L. Lin, Z. Lei, X. Bi, and H. Yang: IEEE Trans. Dielectr. Electr. Insul. **20** (2013) 2091. https://doi.org/10.1109/TDEI.2013.6678857